PNAS RESEARCH ARTICLE | NEUROSCIENCE
PSYCHOLOGICAL AND COGNITIVE SCIENCES OPEN ACCESS

Human cerebellum and corticocerebellar connections involved in emotional memory enhancement

Matthias Fastenrath[a,b], Klara Spalek[a,b,c,d], David Coynel[a,b], Eva Loos[a,b], Annette Milnik[b,c], Tobias Egli[b,c], Nathalie Schicktanz[a,b], Léonie Geissmann[a,b], Benno Roozendaal[d], Andreas Papassotiropoulos[b,c,e,f,1], and Dominique J.-F. de Quervain[a,b,e,1,2]

Edited by James McGaugh, University of California Irvine, Irvine, CA; received March 21, 2022; accepted August 9, 2022

Emotional information is better remembered than neutral information. Extensive evidence indicates that the amygdala and its interactions with other cerebral regions play an important role in the memory-enhancing effect of emotional arousal. While the cerebellum has been found to be involved in fear conditioning, its role in emotional enhancement of episodic memory is less clear. To address this issue, we used a whole-brain functional MRI approach in 1,418 healthy participants. First, we identified clusters significantly activated during enhanced memory encoding of negative and positive emotional pictures. In addition to the well-known emotional memory–related cerebral regions, we identified a cluster in the cerebellum. We then used dynamic causal modeling and identified several cerebellar connections with increased connection strength corresponding to enhanced emotional memory, including one to a cluster covering the amygdala and hippocampus, and bidirectional connections with a cluster covering the anterior cingulate cortex. The present findings indicate that the cerebellum is an integral part of a network involved in emotional enhancement of episodic memory.

cerebellum | dynamic causal modeling | emotional memory enhancement | episodic memory | fMRI

Significance

Enhanced memory for emotional stimuli is crucial for survival, but it may also contribute to the development and maintenance of fear-related disorders in case of highly aversive experiences. This large-scale functional brain imaging study identifies the cerebellum and cerebellar–cerebral connections involved in the phenomenon of superior memory for emotionally arousing visual information. These findings expand knowledge on the role of the cerebellum in complex cognitive and emotional processes and may be relevant for the understanding of psychiatric disorders with aberrant emotional circuitry, such as posttraumatic stress disorder or autism spectrum disorder.

Enhanced memory for emotionally arousing information is a well-recognized phenomenon that has adaptive value in evolutionary terms, as it is vital to remember both dangerous and favorable situations (1, 2). From studies in rodents, it is well established that emotional arousal leads to noradrenergic activation of the amygdala, which in turn activates the hippocampus and other brain regions to enhance memory consolidation of emotionally arousing information (3–5). Moreover, there is evidence from human studies that emotional arousal and noradrenergic activation already regulate memory processes during encoding (6–10) and that the connection strength from the amygdala to the hippocampus is rapidly increased during the encoding of emotionally arousing information compared to neutral information (11). Apart from the amygdala and hippocampus, two meta-analyses of human brain activation studies using functional MRI (fMRI) indicated the potential relevance of several additional brain regions for enhanced encoding of declarative memory by emotional arousal, including the middle occipital gyrus, middle frontal gyrus, fusiform gyrus, inferior frontal gyrus, supramarginal gyrus, orbitofrontal cortex, parietal cortex, claustrum, caudate, and the insula (12, 13). Even though the cerebellum has been occasionally listed in fMRI studies on emotional memory enhancement (14, 15), a meta-analysis including 15 studies did not list it (12). A more recent meta-analysis including 25 studies did find the cerebellum to be significantly activated, but after excluding three studies showing no behavioral enhancement effect, the significance vanished (13). Potential reasons for this ambiguity include that the cerebellum may have shown only subthreshold significance levels in individual studies or that the cerebellum has a priori not been included in the analysis (16).

The cerebellum is typically known for its important role in controlling motor functions (17). However, there is evidence that the outputs of the cerebellum target not only cortical motor areas but also several nonmotor cortical and subcortical regions that are involved in higher brain functions, including emotion and cognition (18–21), and that the cerebellum itself holds robust representations of multiple networks involved in these functions (22, 23). Notably, it is known from animal and human studies that the cerebellum plays an important role in fear conditioning (19, 24–27), which is traditionally categorized as an unconscious or nondeclarative form of learning with a strong emotional component (5, 28). It is less clear, however, whether the cerebellum is also involved in the enhancing effect of emotional arousal on episodic memory, a declarative form of memory that requires conscious memory encoding and enables the conscious recollection of information along with its context (5, 29, 30). Animal and human lesion studies and human neuroimaging studies indicate that fear conditioning and emotional enhancement of episodic memory partly depend on the

Author affiliations: [a]Division of Cognitive Neuroscience, Faculty of Medicine, University of Basel, Basel, 4055, Switzerland; [b]Research Platform Molecular and Cognitive Neurosciences, University of Basel, Basel, 4055, Switzerland; [c]Division of Molecular Neuroscience, Faculty of Medicine, University of Basel, Basel, 4055, Switzerland; [d]Department of Cognitive Neuroscience, Radboud University Medical Center, Donders Institute for Brain, Cognition and Behaviour, Radboud University, Nijmegen, 6525, The Netherlands; [e]Psychiatric University Clinics, University of Basel, Basel, 4002, Switzerland; and [f]Department Biozentrum, Life Sciences Training Facility, University of Basel, Basel, 4056, Switzerland

Author contributions: M.F., A.P., and D.J.-F.d.Q. designed research; K.S. and E.L. performed research; M.F., D.C., and D.J.-F.d.Q. analyzed data; and M.F., K.S., D.C., E.L., A.M., T.E., N.S., L.G., B.R., A.P., and D.J.-F.d.Q. wrote the paper.

The authors declare no competing interest.

This article is a PNAS Direct Submission.

[1]A.P. and D.J.-F.d.Q. jointly supervised this work.

[2]To whom correspondence may be addressed. Email: dominique.dequervain@unibas.ch.

This article contains supporting information online at http://www.pnas.org/lookup/suppl/doi:10.1073/pnas.2204900119/-/DCSupplemental.

Published October 3, 2022.

same neural underpinnings, such as the amygdala (5, 12, 31, 32). Therefore, it is possible that the cerebellum is involved not only in fear conditioning but also in emotional enhancement of episodic memory. In the present study, we investigated whether the cerebellum and cerebellar–cerebral connections are involved in the phenomenon of superior episodic memory for emotionally arousing visual information.

We used an fMRI sample of 1,418 healthy human participants who performed a picture encoding task containing positive and negative emotional and neutral pictures, followed by a free recall test, which assesses episodic memory (29, 30), 20 min after the end of encoding. While emotional arousal rather than valence has been identified as driving the memory-enhancing effect of salient information on episodic memory (5, 33, 34), valence-related differences have also been identified (35). Here, we focused on the identification of emotional arousal effects common to positive and negative valence. The large sample size allowed us to divide the sample into a discovery ($n = 945$ participants) and replication sample ($n = 473$ participants; see *Materials and Methods*). To measure the neural correlates of superior memory for emotional information during encoding, we used the subsequent emotional memory paradigm (12). This paradigm assesses the difference between the encoding activity of later successfully recalled emotional items versus that of nonrecalled emotional items, compared to successfully recalled neutral items vs. nonrecalled neutral items (termed "enhanced emotional memory encoding"). At first, we identified voxels with significantly increased activity during enhanced emotional memory encoding in the discovery sample. We performed this analysis for the entire brain, including the cerebellum. From the voxels that showed increased activity during enhanced emotional memory encoding, we defined regions of interest (ROIs). We defined ROIs functionally, rather than anatomically, as the sensitivity of detecting the presence of connections can be increased by using ROIs that match actual functional boundaries (36). Specifically, we combined voxels with a similar response profile to create spatially coherent and temporal homogeneous ROIs by using a clustering approach (37). We then tested whether the identified ROIs showed increased activity during enhanced emotional memory encoding also in the replication sample.

With the replicated ROIs (i.e., one cerebellar ROI, 25 cerebral ROIs) we finally explored the directed effective connectivity between the cerebellar ROI and the cerebral ROIs using dynamic causal modeling (DCM) (38, 39) in both samples. Whereas DCM was originally developed to test specific hypotheses concerning the presence, direction, and modulators of effective connectivity between a set of predefined brain regions, it can be also applied in an exploratory manner involving a large number of brain regions and models ([40]; see *Materials and Methods*). Here we applied DCM to explore the directed effective connectivity between the cerebellar ROI and the cerebral ROIs involved in emotional memory enhancement. DCM allowed us to determine 1) whether the strength of those connections was increased during successful emotional memory encoding, and 2) the direction of effective connectivity to learn whether the input from the cerebellum causally drives a cerebral ROI implicated in emotional memory enhancement or if the direction of influence is the other way around.

Results

Behavioral data: Emotional memory enhancement. The behavioral results in both the discovery and replication sample indicated that participants freely recalled more emotional (positive and negative) pictures than neutral pictures (discovery sample, mean difference: 4.50 ± 2.76 [mean ± SD], $T = 50.01$, $P = 7.53 \times 10^{-268}$, $n = 945$; replication sample, mean difference: 4.65 ± 2.60 [mean ± SD], $T = 38.82$, $P = 7.03 \times 10^{-149}$, $n = 473$). For a detailed description of the behavioral data, see reference (11). This emotional memory enhancement was not significantly associated with age or sex ($P > 0.05$; 2-sided).

Activity related to enhanced emotional memory encoding. For the contrast representing enhanced emotional memory encoding, 7,708 voxels with increased activity were identified in the discovery sample at a whole-brain level, corrected for multiple comparisons using the family-wise error (FWE) rate procedure ($n = 944$, $P_{\text{whole-brain-FWE-corrected}} < 0.05$; *SI Appendix*, Fig. S2 and Table S3). We did not observe significant positive or negative associations between activity and the effects of sex, age, changes in scanner software, or changes in gradient coils ($P_{\text{whole-brain-FWE-corrected}} > 0.05$). Voxels related to enhanced emotional memory encoding were parcellated into 30 clusters (i.e., ROIs) to reduce the dimensionality of the data (Fig. 1 and *SI Appendix*, Figs. S3–S7, see *Materials and Methods* for details on the parcellation method). One cluster (ROI 11) contained isolated voxels and small clusters of voxels that were not spatially coherent and was therefore removed from further analysis.

Out of the 29 remaining ROIs, 28 were located in neocortical and subcortical regions of the cerebrum and one was in the cerebellum (Fig. 1; see *SI Appendix*, Table S5 for details on the number of voxels as well as the anatomical correspondence per cluster). According to a probabilistic magnetic resonance (MR) atlas of the human cerebellum (41), the cerebellar cluster in the discovery sample mapped mainly onto the vermis of the cerebellum (local maximum by 76% in lobule IX, and by 22% in the replication sample). Out of the 29 ROIs identified in the discovery sample, 26 ROIs (including the cerebellum) were also significantly activated during enhanced emotional memory encoding in the replication sample (significance threshold for ROI maxima: $T = 4.41$, $P < 0.05$, one-sided, Bonferroni-corrected for all significant voxels of the 29 ROIs identified in the discovery sample). Maxima for ROIs 7, 13, and 25 did not reach significance in the replication sample and therefore, these ROIs were not considered for the DCM analysis. In summary, the replicated 26 ROIs mapped onto the occipital, temporal, parietal, and frontal cortex and onto the amygdala/hippocampus, cingulate, thalamus, brainstem, and cerebellum (Fig. 1; *SI Appendix*, Table S5).

Notably, activity related to successful memory encoding did not significantly differ between the positive and negative pictures in the cerebellar ROI in both the discovery and the replication samples ($P_{\text{whole-brain-FWE-corrected}} > 0.05$, $P_{\text{small-volume-corrected}} > 0.001$).

DCM: Connection strength during enhanced emotional memory encoding. The replicated 26 ROIs related to enhanced emotional memory encoding entered the DCM analysis. To investigate changes in connection strength during enhanced emotional memory encoding between the cerebellar ROI and the remaining 25 cerebral ROIs, we used a series of 2-node (cerebellum to all others) DCMs to explore all pairwise (bidirectional) connections (note that the large number of model parameters precluded the inclusion of all 26 ROIs into a single DCM model).

Within the discovery sample, 25 connections (out of the 50 possible unidirectional connections) showed increased strength during enhanced emotional memory encoding (posterior probability > 0.99). Considering the number of tests, we applied a conservative probability threshold of 0.99 and replicated the results in an independent sample using the same threshold (38, 42, 43). Fifteen out of the 25 connections also had

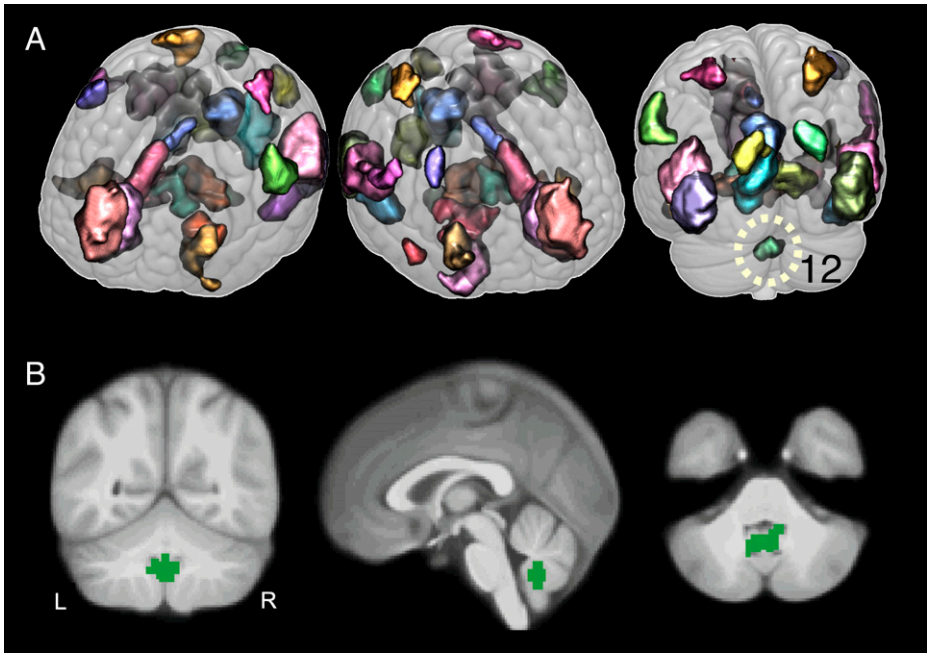

Fig. 1. Clusters showing an increased activation for enhanced emotional memory encoding within the discovery sample. Clusters span voxels significantly activated during enhanced emotional memory encoding ($P_{\text{whole-brain-FWE-corrected}} < 0.05$, $n = 944$). These clusters were used as ROIs to explore the connectivity of the cerebellar cluster (ROI 12). Different colors denote different clusters. (*A*) Three-dimensional images of the 29 clusters. (*B*) Sagittal, coronal, and horizontal views, focusing on the cluster located in the cerebellum (ROI 12). L, left; R, right. See *SI Appendix*, Figs. S3–S7 for additional illustrations.

increased strength in the replication sample (posterior probability > 0.99) (Fig. 2 and *SI Appendix*, Figs. S8–S10). Out of those 15 replicated connections, 11 connections showed increased connection strength from the cerebellum to the cerebral regions. Of particular interest is the strong connection from the cerebellar ROI to ROI 26 that includes voxels from the amygdala and hippocampus (Fig. 2). Four connections showed increased connection strength from the cerebral regions to the cerebellum (Fig. 2). The connections between the cerebellar ROI and ROI 22 that includes voxels from the rostral anterior cingulate ROI and between the cerebellar ROI and ROI 9 that contains voxels from the precentral cortex showed increased strength in both directions.

Discussion

The aim of the present study was to investigate whether the cerebellum and cerebellar–cerebral connections are involved in the phenomenon of superior episodic memory for emotionally arousing visual information. In the first step, we identified clusters showing increased activity during enhanced encoding of emotional pictures. The cerebral clusters mapped onto the occipital, temporal, parietal, and frontal cortex and onto the amygdala/hippocampus, cingulate, and thalamus. These brain activation results are largely in line with the findings of two meta-analyses of enhanced emotional memory encoding in humans (12, 13) and extensive experimental work in animals (4, 32, 44). In addition to these cerebral regions, we found robust evidence for a cluster located mainly within the vermis of the cerebellum showing increased activity during enhanced emotional memory encoding in two large samples. Interestingly, the midline cerebellum has been found to be activated during recall of emotional personal life episodes, indicating a role of this region in emotional memory retrieval (21).

There is accumulating evidence that the cerebellum, in particular the cerebellar vermis, is crucially involved in fear conditioning (19, 24, 26, 27). In rodents, it has been shown that lesions of the vermis abolish heart rate conditioning (45) and that the vermis is necessary for intact fear conditioning (46). In humans, it has been reported that patients with lesions of the cerebellar vermis show impaired acquisition of fear-conditioned bradycardia (47). Moreover, an fMRI study in healthy participants found the vermis to be involved in eye-blink classical conditioning (48). The vermis has efferent projections to limbic regions, including the amygdala and hippocampus, structures involved in delay conditioning and trace conditioning, respectively (49). The connection of the vermis with the amygdala and hippocampus would also allow an influence of the vermis on the enhancement of episodic memories by emotional arousal, which depends on both structures (5). The findings of the present study indeed indicate that the vermis is not only involved in fear conditioning but is also involved in the phenomenon of superior episodic memory of emotionally arousing visual information.

The subsequent DCM connectivity analysis indicated that several cerebellar–cerebral connections showed increased strength during enhanced emotional memory encoding (Fig. 2), suggesting that the cerebellum is an integral component of the network involved in emotional memory enhancement. Specifically, we found 11 connections with increased connection strength from the cerebellum to the cerebral regions. In the context of enhanced emotional memory encoding, the connection to the ROI that includes voxels from the amygdala and hippocampus (ROI 26) seems of special interest. It has been shown that the cerebellum and the amygdala are functionally interconnected during fear conditioning (50, 51). Moreover, studies in rats and cats showed that electrical stimulation of the vermis (outside of a learning context) modulates (i.e., some units are facilitated and others are inhibited) amygdala and hippocampus activity (52, 53), indicating that the vermis is functionally connected with these limbic regions. These findings fit with the direction found in the current DCM analysis, indicating an influence

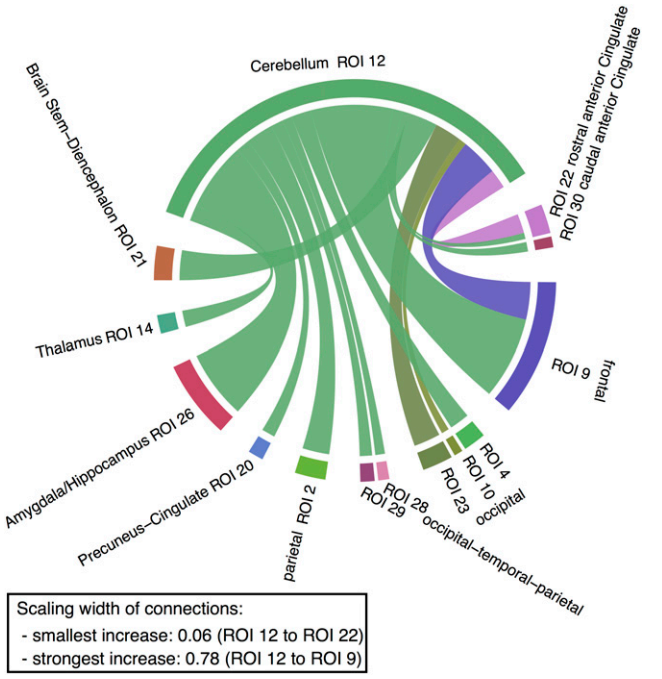

Fig. 2. Increase in the strength of cerebellar connections during enhanced emotional memory encoding. Green edges indicate an increased connection from the cerebellum to a target ROI, while the other colors represent an increased connection from the ROI to the cerebellum. The width of the edges denotes the strength of the increase in connectivity in the replication sample. Only replicating connections are depicted (discovery sample n_{max} = 902, n_{mean} = 887, n_{min} = 798; replication sample n_{max} = 433, n_{mean} = 426, n_{min} = 378; posterior probability > 0.99; *SI Appendix*, Table S1). For a detailed breakdown of anatomical localization per ROI, see *SI Appendix*, Table S5. For connection strength values, see *SI Appendix*, Tables S6–S9. For additional illustrations, see *SI Appendix*, Figs. S8–S10.

of the vermis on ROI 26. There is ample evidence that the amygdala and hippocampus, as well their interactions, are crucially involved in the enhancing effect of emotional arousal on episodic memory (4, 5, 11, 54).

We also found evidence for the involvement of bidirectional connections of the cerebellum with the ROI, which included voxels from the anterior cingulate cortex (ROI 22), in emotional memory enhancement. A resting-state functional connectivity MRI study in healthy humans has shown that the cingulate is functionally connected with the cerebellum (23). Furthermore, the anterior cingulate has been related to emotion, reward valuation, and value representations (55). It has been postulated that the anterior cingulate cortex, in addition to the amygdala and the insula, is a fundamental part of a large-scale salience network that functions to segregate the most relevant among internal and extrapersonal stimuli in order to guide behavior (56, 57). Moreover, the salience network has been reported to be activated by noradrenergic activation (58), a neurotransmitter system crucially involved not only in arousal and attentional processes but also in emotional memory enhancement (59). Interestingly, the locus coeruleus, the principal site for brain synthesis of norepinephrine, also projects to areas throughout the cerebellum (60). Whether the cerebellum gets activated directly by the locus coeruleus or indirectly by the salience network has yet to be determined. Furthermore, we found a bidirectional connection of the cerebellum with the ROI in the frontal cortex (mainly precentral) that may be related to the regulation of motor functions (61), possibly motor learning, in the context of emotional memory enhancement. Finally, we found connections with increased connection strength from two cerebral ROIs to the cerebellum (i.e., ROI 10, including voxels from the lingual and pericalcarine gyrus, and ROI 23, including voxels from the lateral occipital cortex).

Taken together, the DCM analysis has shown that from the 25 cerebral ROIs involved in emotional memory enhancement, 13 ROIs showed increased connection strength with the cerebellum, mostly in the direction from the cerebellum to cortical ROIs, in two cases in the opposite direction and in another two cases in both directions. These findings suggest that the cerebellum is an integral part of a connectivity network involved in emotional memory enhancement. However, from these results we cannot infer which of these connections are the most important ones. Since ROIs were defined functionally, rather than anatomically, we can also not specify the precise anatomical substrates of the cortical ROIs. We have chosen this approach because the sensitivity of detecting the presence of connections can be increased by using ROIs that match functional boundaries (36). The consequence of this procedure is a loss of anatomical specificity and the inability to distinguish between contributions of distinct anatomical structures within a certain ROI. Moreover, since the DCMs tested here included only two nodes, they do not consider whether the influence between the cerebellum and a second ROI is mediated by additional regions. The values of our connectivity parameters therefore potentially reflect both direct and indirect connections.

The current findings may contribute to a better understanding of the network involved in emotional memory enhancement in physiological conditions. Furthermore, the findings may also have implications for understanding pathological conditions, such as posttraumatic stress disorder (PTSD), since the formation of an excessively strong aversive-memory trace after a traumatic event is an important pathogenic mechanism in the development of fear-related disorders (1, 62, 63). Whereas it will not be possible to investigate initial memory formation in PTSD by means of fMRI, studies may investigate the neural correlates of traumatic memory retrieval. A recent fMRI study followed this approach and found enhanced brain activation in the cerebellum (including the vermis), occipital gyri, supramarginal gyrus, and amygdala during trauma recall in patients with PTSD (64).

In contrast, cerebellar hypoactivity could be related to conditions with reduced emotional memory enhancement. Indeed, clinical studies indicate that the pathologies affecting vermal functioning are associated with a range of cognitive and emotional impairments, including symptoms of autism spectrum disorder (65, 66). Interestingly, patients with autism spectrum disorder show deficits in emotional enhancement of episodic memories (67, 68). It is possible that these deficits partially originate from structural and functional abnormalities of the amygdala often observed in this disorder (69, 70). However, based on the present results, the vermal hypoplasia in autism spectrum disorder may also contribute to impaired emotional enhancement of episodic memory. This hypothesis would need to be tested in patients with autism with varying degrees of amygdala and vermis abnormalities.

There is mounting evidence indicating that the cerebellum, in particular the cerebellar vermis, and its connections to several cerebral regions, including the limbic system, are involved in emotional functions, including emotional perception, emotional recognition, emotional processing, and fear conditioning (27, 71). The present findings now suggest that the cerebellum is also part of a circuitry involved in the emotional enhancement of episodic memory. Within this circuitry, the cerebellum receives input from several cerebral regions including the

cingulate, while the amygdala/hippocampus and several other brain regions receive input from the cerebellum. These findings expand knowledge about the role of the cerebellum in complex cognitive and emotional processes and may be relevant for the understanding of psychiatric disorders with aberrant emotional circuitry, such as PTSD or autism spectrum disorder.

Materials and Methods

Participants. We recruited healthy, young participants (872 females, 546 males, mean age = 22.39 y, SD = 3.27). Advertising was done mainly at the University of Basel and in local newspapers. The participants were free of any neurological or psychiatric illness, did not take any medication at the time of the experiment (except hormonal contraceptives), and were between ages 18 and 35 y. Physical and mental health was assessed based on standard questionnaires. The experiment was approved by the ethics committee of the Canton of Basel, Switzerland. All participants gave written informed consent before participating in the study. Prior to the analysis, the sample was divided into a discovery sample ($n = 945$, 2/3 of all participants) and a replication sample ($n = 473$, 1/3 of all participants) by randomly assigning participants to one of the samples. Randomization was performed using the Matlab function randperm. There were no significant differences between the discovery and replication samples in terms of age, sex, or emotional memory enhancement ($P \geq 0.33$, 2-sided testing, $n = 1{,}418$).

Experiment: Procedure. Participants underwent four consecutive tasks: a picture-encoding task, a working-memory task, a free-recall memory test, and a recognition task. Participants were first instructed and then trained on the picture-encoding and working-memory tasks. After training, they were positioned in the scanner and received earplugs and headphones to reduce scanner noise. Their heads were fixated in the coil using small cushions, and they were told not to move. Pictures were presented in the scanner using MR-compatible liquid crystal display goggles (VisualSystem; NordicNeuroLab, Bergen, Norway). Eye correction was used when necessary. The picture-encoding task lasted for ∼20 min. Immediately afterward, participants performed a letter n-back (0-back and 2-back conditions) working-memory task in the scanner for ∼10 min. In the current study, the working-memory task was used as a distraction task between encoding and recall of memory testing. Hence, we did not analyze the data from the working-memory task itself (see reference 72 for a description of the task). After leaving the scanner, participants were given an unannounced free-recall memory test of the pictures in a separate room (no time limit was set for this task). After the free recall, participants were repositioned in the scanner and performed a recognition task (see reference 73 for a description of the task). Participants received 25 Swiss francs/h for participation. Due to organizational constraints, we had to change the room in which pictures were recalled, which meant that some participants recalled pictures in a slightly different setting.

Experiment: Design of picture-encoding task. Stimuli consisted of 72 pictures (24 positive, 24 negative, and 24 neutral) that were selected from the International Affective Picture System (IAPS) (74) and from in-house standardized picture sets that allowed us to equate the pictures for visual complexity and content (e.g., human presence). Pictures received from the IAPS were classified according to the IAPS valence rating. Eight out of the 24 neutral pictures were not received from the IAPS. These pictures were rated based on an in-house valence rating (11). Based on normative valence scores (from 1 to 9), pictures were assigned to negative (2.3 ± 0.6), neutral (5.0 ± 0.3), and positive (7.6 ± 0.4) conditions, resulting in 24 pictures for each valence. Positive stimuli were initially selected to match arousal ratings of negative stimuli based on data of a pilot study in 20 participants not included in the study. Four additional pictures showing neutral objects were presented. Two of these pictures were presented in the beginning and two at the end of the picture task. These pictures were excluded from recall performance evaluation to control for primacy and recency effects in memory. Examples of pictures included erotica, sports, and appealing animals for the positive valence; bodily injury, snakes, and attack scenes for the negative valence; and neutral faces, household objects, and buildings for the neutral condition. In addition, 24 scrambled pictures were used. The background of the scrambled pictures contained the color information of all pictures used in the experiment (except primacy and recency pictures), overlaid with a crystal and distortion filter (Adobe Photoshop CS3). In the foreground, a mostly transparent geometric object (a rectangle or ellipse of differing size and orientation) was shown. For the present study, the scrambled pictures were of no interest.

The pictures were presented for 2.5 s in a quasi-randomized order so that at maximum four pictures of the same category occurred consecutively. A fixation cross appeared on the screen for 500 ms before each picture presentation. The stimulus onset time was jittered within 3 s (1 repetition time [TR]) per valence category with regard to the scan onset. During the intertrial period, participants rated each of the 72 pictures according to valence (negative, neutral, or positive) and arousal (large, medium, or small) on a 3-point scale (self-assessment manikin) by pressing a button with their dominant hand. For scrambled pictures, participants rated the form (vertical, symmetrical, or horizontal) and size (large, medium, or small) of the geometric object in the foreground. The software Presentation (Neurobehavioral Systems, Inc., Berkeley, CA; https://www.neurobs.com) was used for the picture presentation.

Behavioral data: Emotional memory enhancement. To document free recall, participants had to write down a description of the recalled pictures. A picture was scored as correctly recalled if the rater could identify the presented picture on the basis of the participant's description. Two trained investigators independently rated the descriptions for recall success (interrater reliability > 99%). A third independent rater decided on pictures that were rated differently. For each participant, we computed how often emotional pictures were recalled compared to neutral pictures: ([recalled positive – recalled neutral] + [recalled negative – recalled neutral])/2. Data points were plotted and were found to be approximately normally distributed (*SI Appendix*, Fig. S1). Two-sided *t* tests were applied to test whether emotional memory performance was significantly different from zero. In addition, we tested for the effects of potential confounders. We used a 2-sample *t* test to assess whether emotional memory performance depended on sex. We used Pearson's linear correlation coefficients to associate recall performance with age. Two-sided *t* tests were applied to test whether the correlation coefficient was significantly different from zero.

Imaging: MRI acquisition. Measurements were performed on a Siemens Magnetom Verio 3 T whole-body MR unit equipped with a 12-channel head coil. Functional time series were acquired with a single-shot echo-planar sequence using parallel imaging (GRAPPA). We used the following acquisition parameters: echo time (TE) = 35 ms; field of view (FOV) = 22 cm; acquisition matrix = 80 × 80, interpolated to 128 × 128; voxel size = 2.75 × 2.75 × 4 mm^3; GRAPPA acceleration factor $R = 2.0$. Using a midsagittal scout image, 32 contiguous axial slices placed along the anterior–posterior commissure plane covering the entire brain with a TR = 3,000 ms ($\alpha = 82°$) were acquired using an ascending interleaved sequence. The first two acquisitions were discarded due to T1 time constant saturation effects. A high-resolution T1-weighted anatomical image was acquired using a magnetization prepared gradient echo sequence (TR = 2,000 ms; TE = 3.37 ms; TI = 1,000 ms; flip angle = 8°; 176 slices; FOV = 256 mm; voxel size = 1 × 1 x 1 mm^3).

Imaging: Software package for statistical analysis of imaging data. We used the statistical parametric mapping (SPM) software SPM12 version 6685 (Wellcome Trust Centre for Neuroimaging, London, UK; https://www.fil.ion.ucl.ac.uk/spm/) implemented in Matlab R2016a.

Imaging: Preprocessing and normalization of echo planar imaging (EPI) volumes. Volumes were slice-time–corrected to the first slice, realigned using the "register to mean" option, and coregistered to the anatomical image by applying a normalized mutual information three-dimensional rigid-body transformation. Successful coregistration was visually verified for each participant. Each volume was masked with the participant's T1 anatomical image to exclude voxels outside of the brain. The echo planar imaging (EPI) volumes were normalized to Montreal Neurological Institute (MNI) space and smoothed with an 8 mm full width at half-maximum (FWHM) Gaussian kernel by applying DARTEL, which led to an improved registration between participants (75, 76).

The interleaved sequence used to acquire functional time series made it a prerequisite to use slice-time correction as a first preprocessing step (77). Slice-timing correction methods can successfully compensate for slice-timing effects (78). Notably, in DCM for fMRI, the direction of causality is not identified by

temporal precedence. Instead, causality is embodied by the mathematical form of the differential state equation of each region. The state equations of a given model define the systems structure (e.g., the connectivity between regions), prescribing explicitly how dynamics arise within the system (39). Therefore, a number of DCM studies with similar TRs were previously conducted (79–81).

Imaging: Modeling of voxel-wise activity. General linear models (GLMs) were specified for each participant to identify voxels activated by task. Regressors modeling the onsets and duration of stimulus events were convolved with a canonical hemodynamic response function. More precisely, the model comprised regressors for button presses modeled as stick/delta functions, picture presentations (positive, neutral, negative, scrambled, primacy, and recency) modeled with an epoch/boxcar function (duration: 2.5 s), and rating scales modeled with an epoch/boxcar function of variable duration (depending on when the subsequent button press occurred). Serial correlations were removed using a first-order autoregressive model, and a high-pass filter (128 s) was applied to remove low-frequency noise. Six movement parameters were also entered as nuisance covariates. We defined two different types of GLMs. One type of GLM was used to identify voxels related to successful emotional memory encoding. Here, positive, negative, and neutral stimuli were modeled separately depending on whether they were subsequently recalled or not. The resulting parameter estimates were contrasted to identify voxels associated with successful emotional memory encoding ([recalled emotional pictures – nonrecalled emotional pictures] – [recalled neutral pictures – nonrecalled neutral pictures]). This contrast was available in 944 out of the 945 participants of the discovery sample (1 subject did not recall any neutral pictures) and in 470 out of the 473 participants of the replication sample (3 subjects did not recall any neutral pictures). To investigate potential valence-related effects in cerebellar activity, we furthermore compared whether activity related to successful memory encoding differed between positive and negative pictures. This corresponded to the following contrast: ([recalled negative pictures – nonrecalled negative pictures] – [recalled positive pictures – nonrecalled positive pictures]). Another type of GLM was specified to identify voxels associated with the encoding of emotional pictures, irrespective of memory. We specified regressors for positive, neutral, and negative pictures, irrespective of whether the pictures were recalled or not, and contrasted the resulting parameter estimates (emotional pictures – neutral pictures). We applied family-wise error (FWE) correction for multiple comparison at the whole-brain level to all contrasts ($P_{\text{whole-brain-FWE-corrected}} < 0.05$). Correction for multiple comparison at the cluster level was applied to test for valence-related effects in the cerebellar cluster ($P_{\text{small-volume-corrected}} < 0.001$, cluster extent $k = 10$).

Imaging: Group statistics of voxel-wise activity. To determine activity related to "successful emotional memory encoding" and to "encoding of emotional pictures," contrast maps were entered in a random-effects model (second-level analysis) using GLM Flex (Martinos Center and Massachusetts General Hospital, Charlestown, MA; https://habs.mgh.harvard.edu/researchers/data-tools/glm-flex-fast2/). We controlled for the effect of sex, age, one change in scanner software, and two changes in gradient coils by including them as covariates. We used GLM Flex because EPI sequences suffer from signal loss in the presence of magnetic-field inhomogeneities that can occur close to air-tissue boundaries. The normalization procedure applied in DARTEL accurately transformed both voxels with signal and voxels with signal loss to MNI space. In SPM, signal loss at an MNI coordinate in a functional image of only one participant led to the exclusion of the voxel at this coordinate from the group-level analysis. Consequently, the probability of a voxel being excluded increased with sample size. GLM Flex circumvented this problem by allowing a variable number of participants at each voxel. The minimum number of participants per voxel was set to 2/3 of all participants.

Imaging: Definition of ROIs—Functionally defined mask. Because the sensitivity of detecting the presence of connections can be increased by using ROIs that match actual functional boundaries (36), we defined ROIs functionally, rather than anatomically. Specifically, within the discovery sample ($n = 945$), we used a functionally derived mask and then used a data-driven, group-level clustering approach to parcellate preprocessed and normalized EPI volumes into spatially coherent and temporal homogeneous regions (37). The mask consisted of voxels that were positively associated with successful emotional memory encoding within the discovery sample ($P_{\text{whole-brain-FWE-corrected}} < 0.05$). The identified voxels were then additionally masked with the encoding of emotional pictures contrast ($P_{\text{whole-brain-FWE-corrected}} < 0.05$) to assure that all included voxels also showed a positive effect for emotion encoding (99% of all voxels significant in the "successful emotional memory encoding contrast" were also significant in the "encoding of emotional pictures contrast").

Imaging: Definition of ROIs—Parcellation procedure. Voxels within the functionally defined mask were combined into ROIs such that the similarity between voxels within the same cluster was maximized compared to the similarity between voxels in different clusters, using a normalized cut method incorporating a spatial constraint (37). For computational expedience, parcellation was performed based on the EPI volumes of 200 participants who were randomly drawn from the discovery sample. These volumes were smoothed with a 6 mm FWHM Gaussian kernel in line with a recent paper (37). Clustering was first performed within each participant, followed by a second-level group clustering, as recommended by Craddock et al. (37). We parcellated the voxels within the mask into 30 ROIs, as we found that this number leads to sufficient spatial specificity while still being manageable with regard to the computational burden induced by the computation of connectivity with DCM. One of these ROIs contained isolated voxels and discrete small clusters that were not spatially coherent. This ROI (ROI 11), which contained 60 voxels, was thus removed from further analysis.

Connectivity analysis: Time-course extraction. We extracted time courses per participant and ROIs from unsmoothed and unnormalized data using the procedure described below. Note that we extracted from unsmoothed data because smoothing can be damaging to connectivity estimation as it leads to a mixing of blood oxygenation level–dependent time courses between regions in close proximity (36).

1. Mapping functional ROIs from MNI space to native participant space: The ROIs as determined in the parcellation procedure were generated in MNI space. We therefore mapped their location to native participant space by inverting the normalization warp field of each participant.
2. Time-course extraction from functional ROIs: Before the actual modeling of connectivity within the DCM framework, participant-specific time courses were extracted from each ROI. The goal of this step was to extract time courses from activated voxels at the single-participant level. The effect size of the encoding of emotional pictures contrast was considerably larger than the effect size of the successful emotional memory contrast, making the former more suitable for distinguishing task-related voxels from voxels without relevant signal at the single-participant level. At the group level, all areas included in this analysis were significantly associated with successful emotional memory encoding, assuring that all ROIs were relevant for successful emotional memory encoding. For each ROI and participant, we consequently identified significant voxels for the emotional > neutral contrast, at an uncorrected threshold of $P < 0.05$, with a minimum cluster size of three voxels. A summary time course was extracted from all those voxels using SPM's "Volume of Interest" extraction tool. In detail, for all selected voxels within an ROI, a PCA was performed. Time points were the observations and voxels were the variables. The PCA returned a series of components ordered by the proportion of variance that each component explained. Each component was associated with a vector of weights (one value per voxel), reflecting the contribution of each voxel to that component. The first eigenvariate reflected the time course of the main component that contributed to a region's response and was selected as a representative time course for the ROI. The time courses were corrected for movement artifacts by adding movement parameters as covariates into the linear model.

Across all 29 functional ROIs, time courses were successfully extracted in 97.88% of all cases in the discovery sample, and in 97.57% of all cases in the replication sample, as they showed robust task-dependent activation in accordance with our significance threshold outlined above. Data from all ROIs in all participants were a prerequisite to run DCM, as the purpose of DCM is to compare different models for an observed activation (38, 39). Hence, we excluded a participant from a particular DCM if a ROI did not show activation in line with the criteria defined above. Out of all ROIs, ROI 9 showed the smallest proportion of participants with robust activation (discovery sample 88.36%; replication sample 85.84%). See *SI Appendix*, Table S1 for the number of participants per DCM and *SI Appendix*, Table S2 for percentages of excluded participants per ROI.

Potential reasons for the lack of sufficiently strong activation in some participants pertained to noise in the data or data loss but may also reflect the use of different cognitive strategies.

Connectivity analysis: DCM. DCM can be applied to test specific hypotheses concerning the presence, direction, and modulators of effective connectivity between a set of predefined brain regions. DCM is described in detail elsewhere (38, 39). In brief, neural interactions between regions are expressed by differential equations, which describe 1) how the activity in one brain region causes dynamics (i.e., rate of change) in another brain region and 2) how these interactions change under the influence of experimental conditions. Here, we compared conditions for emotional and neutral pictures while considering whether a picture was later recalled or not. DCM strives for neurophysiological interpretability by making an explicit distinction between the "neural level" and the "hemodynamic level" (82). This is achieved by inverting a biophysically motivated and parameterized forward model that links the modeled neural dynamics to the measured hemodynamic time courses (38). The connectivity parameters can therefore be interpreted as an influence between neural populations (39). Our inference on connectivity depended on the underlying mathematical assumptions incorporated in the parameterization of DCM. These assumptions have been critically assessed (83).

We chose DCM over other methods because it offers several advantages. DCM infers connectivity by modeling neural dynamics with a system of differential equations. Therefore, the direction of influence and the condition-dependent modulation of connection strength can be more meaningfully determined than with static connectivity models such as correlation or structural equation modeling (82, 84, 85).

Connectivity analysis: DCM—Model space. We used a posthoc model selection procedure, which requires the estimation of only one full model to find the model evidence for all possible connection architectures (40), thereby performing an exhaustive model comparison. We used this selection procedure rather than a traditional comparison of a limited number of a priori models because this algorithm greatly reduces the computational burden by approximating the connectivity parameters of nested submodels from the inference on one full model. Although it would have been interesting to include all 26 clusters into one single model, this was computationally not feasible. We explored all pairwise connections between the cerebellar ROI and the remaining 25 ROIs by defining a series of 2-node DCMs where the ROI located in the cerebellum was systematically paired with one of the other ROIs. Connectivity parameters represent the net connectivity between ROIs–i.e., they do not consider whether or not the influence between two ROIs is mediated by additional regions, unless these additional regions are explicitly included in the DCM model. Since the DCMs tested here included only two nodes, they did not examine whether the influence between the cerebellum and a second ROI was mediated by additional regions. The values of our connectivity parameters therefore potentially reflected both direct and indirect connections.

We applied bilinear, deterministic DCM with two states (version DCM12) (86). We specified reciprocal intrinsic connections between each ROI. Extrinsic inputs to ROIs drive the network and quantify how ROIs respond to external stimuli. Four different input regressors were defined, containing 1) emotional and neutral pictures, 2) scrambled pictures, 3) button presses, and 4) rating scale presentation. Each of the input regressors could enter the network at all ROIs. The strength of the intrinsic connections between ROIs could be modulated by the following conditions: emotional recalled pictures, emotional nonrecalled pictures, neutral recalled pictures, and neutral nonrecalled pictures.

For a Bayesian perspective on multiple comparison, see references (87, 88). Notably, we replicated the results of the discovery sample in a second sample.

Connectivity analysis: DCM—Model estimation. We used an efficient posthoc model selection that required the estimation of only one full model to find 1) the model evidence for all possible connection architectures with Bayesian model selection (BMS), 2) posterior probabilities resulting from family-level inferences to determine the probability for a contrast of parameter estimates, and 3) Bayesian parameter averages over all possible models showing whether a contrast of parameter estimates differed from zero (40, 84, 89). Because we used fixed-effects BMS, we assumed that the optimal model was the same for each participant in the population (39). Estimation of DCM models was performed at the sciCORE (https://scicore.unibas.ch/) scientific computing core facility at University of Basel.

Connectivity analysis: DCM—Parameter analysis. We used Bayesian inference to assess whether connection strength was increased during successful emotional memory encoding. Specifically, we used the posterior expectations and posterior covariances to compute the posterior probability that the contrast between modulators of connection strength was bigger than zero. The contrast for successful emotional memory encoding was built by subtracting the modulators of the following conditions: (recalled emotional pictures – nonrecalled emotional pictures) – (recalled neutral pictures – nonrecalled neutral pictures). First, within the discovery sample, we identified those connections that had a posterior probability of contrast greater than 0.99. Second, we analyzed these connections in the replication sample, testing whether they too had a posterior probability of contrast greater than 0.99. In descriptive terms, the applied probability threshold of 0.99 can be interpreted as providing very strong evidence for an effect (42, 43). We focused on increases rather than decreases in connection strength, since ROIs were defined based on voxels with increased activity.

Calculations with regard to connection strength were based on the strength of the contrast in the replication sample. Connections were visualized using the circlize library in R (90).

Segmentation of anatomical image. Each participant's anatomical image was automatically segmented into cortical and subcortical structures using FreeSurfer version 4.5 (91). Labeling of the cortical gyri was based on the Desikan–Killiany atlas (92), yielding 35 cortical and seven subcortical regions per hemisphere. Note that the applied segmentation and labeling technique provides an accuracy comparable to manual labeling by experts (91, 92).

Anatomical localization of ROIs based on a population-averaged anatomical probabilistic atlas. Segmentations of cortical and subcortical structures retrieved from FreeSurfer (see paragraph above) were used to build a population-average probabilistic anatomical atlas, based on data of 1,000 out of the 1,418 participants. Individual segmented anatomical images were normalized to the study-specific anatomical template space using the participants' previously computed warp field and were affine-registered to the MNI space. Nearest-neighbor interpolation was applied to preserve the labeling of the different structures. The normalized segmentations were finally averaged across participants to create a population-average probabilistic atlas. Each voxel of the template could consequently be assigned a probability of belonging to a given anatomical structure.

This population-average probabilistic atlas was used to report the anatomical location of coordinates and ROIs. Percentages per coordinate denoted the population-average probability of an anatomical label. Furthermore, we reported the average percentage of regional correspondence per ROI. Per ROI, we determined which anatomical labels were spanned by its voxels. We then summed up the probabilities per label across all voxels within the ROI and divided the sum by the overall number of voxels in the mask. A 100% correspondence would occur if all voxels of a ROI were located within the same anatomical region, and each voxel itself had a probability of 100% of being located in this region.

Data, Materials, and Software Availability. Individual, first-level maps for the two contrasts of interest (successful emotional memory encoding and encoding of emotional pictures) are available in the Open Science Framework (OSF, https://osf.io/ghtvy) (93), together with the individual covariates. Individual first-level and VOI files are available on Figshare (https://figshare.com/projects/CB-DCM/149317) (94). The corresponding unthresholded group-level maps as well as the binary mask of the functional ROIs have been deposited in Neurovault (https://neurovault.org/collections/12932) (95). The group-level DCM files are available in OSF (https://osf.io/ghtvy) (93).

ACKNOWLEDGMENTS. We thank Elmar Merkle, Christoph Stippich, and Oliver Bieri for granting access to the fMRI facilities of the University Hospital Basel. This work was funded by the Swiss National Science Foundation (Sinergia grant CRSI33_130080 to D.J.-F.d.Q. and A.P.). M.F. was funded by the Research Fund for Junior Researchers of the University of Basel (grant DPE2141). Calculations were performed at the sciCORE (https://scicore.unibas.ch/) scientific computing core facility at University of Basel. The authors declare no competing financial interests.

1. D. de Quervain, L. Schwabe, B. Roozendaal, Stress, glucocorticoids and memory: Implications for treating fear-related disorders. *Nat. Rev. Neurosci.* **18**, 7–19 (2017).
2. J. L. McGaugh, *The Making of Lasting Memory* (Weidenfeld & Nicolson, 2003).
3. J. L. McGaugh, Memory–A century of consolidation. *Science* **287**, 248–251 (2000).
4. B. Roozendaal, J. L. McGaugh, Memory modulation. *Behav. Neurosci.* **125**, 797–824 (2011).
5. K. S. LaBar, R. Cabeza, Cognitive neuroscience of emotional memory. *Nat. Rev. Neurosci.* **7**, 54–64 (2006).
6. S. B. Hamann, T. D. Ely, S. T. Grafton, C. D. Kilts, Amygdala activity related to enhanced memory for pleasant and aversive stimuli. *Nat. Neurosci.* **2**, 289–293 (1999).
7. T. Canli, Z. Zhao, J. Brewer, J. D. E. Gabrieli, L. Cahill, Event-related activation in the human amygdala associates with later memory for individual emotional experience. *J. Neurosci.* **20**, RC99 (2000).
8. A. H. van Stegeren *et al.*, Noradrenaline mediates amygdala activation in men and women during encoding of emotional material. *Neuroimage* **24**, 898–909 (2005).
9. M. W. Cole *et al.*, Multi-task connectivity reveals flexible hubs for adaptive task control. *Nat. Neurosci.* **16**, 1348–1355 (2013).
10. R. M. Todd, T. W. Schmitz, J. Susskind, A. K. Anderson, Shared neural substrates of emotionally enhanced perceptual and mnemonic vividness. *Front. Behav. Neurosci.* **7**, 40 (2013).
11. M. Fastenrath *et al.*, Dynamic modulation of amygdala-hippocampal connectivity by emotional arousal. *J. Neurosci.* **34**, 13935–13947 (2014).
12. V. P. Murty, M. Ritchey, R. A. Adcock, K. S. LaBar, fMRI studies of successful emotional memory encoding: A quantitative meta-analysis. *Neuropsychologia* **48**, 3459–3469 (2010).
13. K. Dahlgren, C. Ferris, S. Hamann, Neural correlates of successful emotional episodic encoding and retrieval: An SDM meta-analysis of neuroimaging studies. *Neuropsychologia* **143**, 107495 (2020).
14. K. R. Mickley Steinmetz, E. A. Kensinger, The effects of valence and arousal on the neural activity leading to subsequent memory. *Psychophysiology* **46**, 1190–1199 (2009).
15. L. Cahill, M. Uncapher, L. Kilpatrick, M. T. Alkire, J. Turner, Sex-related hemispheric lateralization of amygdala function in emotionally influenced memory: An FMRI investigation. *Learn. Mem.* **11**, 261–266 (2004).
16. D. Talmi, A. K. Anderson, L. Riggs, J. B. Caplan, M. Moscovitch, Immediate memory consequences of the effect of emotion on attention to pictures. *Learn. Mem.* **15**, 172–182 (2008).
17. T. Ito, *The Cerebellum and Neural Control* (Raven Press, 1984).
18. P. L. Strick, R. P. Dum, J. A. Fiez, Cerebellum and nonmotor function. *Annu. Rev. Neurosci.* **32**, 413–434 (2009).
19. P. Strata, The emotional cerebellum. *Cerebellum* **14**, 570–577 (2015).
20. L. F. Koziol *et al.*, Consensus paper: The cerebellum's role in movement and cognition. *Cerebellum* **13**, 151–177 (2014).
21. A. R. Damasio *et al.*, Subcortical and cortical brain activity during the feeling of self-generated emotions. *Nat. Neurosci.* **3**, 1049–1056 (2000).
22. A. Xue *et al.*, The detailed organization of the human cerebellum estimated by intrinsic functional connectivity within the individual. *J. Neurophysiol.* **125**, 358–384 (2021).
23. C. Habas *et al.*, Distinct cerebellar contributions to intrinsic connectivity networks. *J. Neurosci.* **29**, 8586–8594 (2009).
24. B. Sacchetti, B. Scelfo, P. Strata, The cerebellum: Synaptic changes and fear conditioning. *Neuroscientist* **11**, 217–227 (2005).
25. I. Lange *et al.*, The anatomy of fear learning in the cerebellum: A systematic meta-analysis. *Neurosci. Biobehav. Rev.* **59**, 83–91 (2015).
26. D. Timmann *et al.*, The human cerebellum contributes to motor, emotional and cognitive associative learning. A review. *Cortex* **46**, 845–857 (2010).
27. M. Adamaszek *et al.*, Consensus paper: Cerebellum and emotion. *Cerebellum* **16**, 552–576 (2017).
28. J. E. LeDoux, Coming to terms with fear. *Proc. Natl. Acad. Sci. U.S.A.* **111**, 2871–2878 (2014).
29. L. R. Squire, S. M. Zola, Episodic memory, semantic memory, and amnesia. *Hippocampus* **8**, 205–211 (1998).
30. E. Tulving, H. J. Markowitsch, Episodic and declarative memory: Role of the hippocampus. *Hippocampus* **8**, 198–204 (1998).
31. J. LeDoux, The emotional brain, fear, and the amygdala. *Cell. Mol. Neurobiol.* **23**, 727–738 (2003).
32. J. L. McGaugh, L. Cahill, B. Roozendaal, Involvement of the amygdala in memory storage: Interaction with other brain systems. *Proc. Natl. Acad. Sci. U.S.A.* **93**, 13508–13514 (1996).
33. M. R. Sutherland, M. Mather, Arousal (but not valence) amplifies the impact of salience. *Cogn. Emotion* **32**, 616–622 (2018).
34. F. Dolcos, K. S. LaBar, R. Cabeza, Dissociable effects of arousal and valence on prefrontal activity indexing emotional evaluation and subsequent memory: An event-related fMRI study. *Neuroimage* **23**, 64–74 (2004).
35. K. R. Mickley Steinmetz, D. R. Addis, E. A. Kensinger, The effect of arousal on the emotional memory network depends on valence. *Neuroimage* **53**, 318–324 (2010).
36. S. M. Smith *et al.*, Network modelling methods for FMRI. *Neuroimage* **54**, 875–891 (2011).
37. R. C. Craddock, G. A. James, P. E. Holtzheimer III, X. P. Hu, H. S. Mayberg, A whole brain fMRI atlas generated via spatially constrained spectral clustering. *Hum. Brain Mapp.* **33**, 1914–1928 (2012).
38. K. J. Friston, L. Harrison, W. Penny, Dynamic causal modelling. *Neuroimage* **19**, 1273–1302 (2003).
39. K. E. Stephan *et al.*, Ten simple rules for dynamic causal modeling. *Neuroimage* **49**, 3099–3109 (2010).
40. M. J. Rosa, K. Friston, W. Penny, Post-hoc selection of dynamic causal models. *J. Neurosci. Methods* **208**, 66–78 (2012).
41. J. Diedrichsen, J. H. Balsters, J. Flavell, E. Cussans, N. Ramnani, A probabilistic MR atlas of the human cerebellum. *Neuroimage* **46**, 39–46 (2009).
42. R. E. Kass, A. E. Raftery, Bayes factors. *J. Am. Stat. Assoc.* **90**, 773–795 (1995).
43. M. E. J. Masson, A tutorial on a practical Bayesian alternative to null-hypothesis significance testing. *Behav. Res. Methods* **43**, 679–690 (2011).
44. E. A. Phelps, J. E. LeDoux, Contributions of the amygdala to emotion processing: From animal models to human behavior. *Neuron* **48**, 175–187 (2005).
45. W. F. Supple Jr., R. N. Leaton, Lesions of the cerebellar vermis and cerebellar hemispheres: Effects on heart rate conditioning in rats. *Behav. Neurosci.* **104**, 934–947 (1990).
46. B. Sacchetti, E. Baldi, C. A. Lorenzini, C. Bucherelli, Cerebellar role in fear-conditioning consolidation. *Proc. Natl. Acad. Sci. U.S.A.* **99**, 8406–8411 (2002).
47. M. Maschke *et al.*, Fear conditioned changes of heart rate in patients with medial cerebellar lesions. *J. Neurol. Neurosurg. Psychiatry* **72**, 116–118 (2002).
48. D. T. Cheng *et al.*, Functional MRI of cerebellar activity during eyeblink classical conditioning in children and adults. *Hum. Brain Mapp.* **35**, 1390–1403 (2014).
49. D. T. Cheng, J. F. Disterhoft, J. M. Power, D. A. Ellis, J. E. Desmond, Neural substrates underlying human delay and trace eyeblink conditioning. *Proc. Natl. Acad. Sci. U.S.A.* **105**, 8108–8113 (2008).
50. B. Sacchetti, T. Sacco, P. Strata, Reversible inactivation of amygdala and cerebellum but not perirhinal cortex impairs reactivated fear memories. *Eur. J. Neurosci.* **25**, 2875–2884 (2007).
51. T. Lee, J. J. Kim, Differential effects of cerebellar, amygdalar, and hippocampal lesions on classical eyeblink conditioning in rats. *J. Neurosci.* **24**, 3242–3250 (2004).
52. R. G. Heath, C. W. Dempesy, C. J. Fontana, W. A. Myers, Cerebellar stimulation: Effects on septal region, hippocampus, and amygdala of cats and rats. *Biol. Psychiatry* **13**, 501–529 (1978).
53. R. G. Heath, Fastigial nucleus connections to the septal region in monkey and cat: A demonstration with evoked potentials of a bilateral pathway. *Biol. Psychiatry* **6**, 193–196 (1973).
54. S. Hamann, Cognitive and neural mechanisms of emotional memory. *Trends Cogn. Sci.* **5**, 394–400 (2001).
55. B. A. Vogt, Submodalities of emotion in the context of cingulate subregions. *Cortex* **59**, 197–202 (2014).
56. W. W. Seeley *et al.*, Dissociable intrinsic connectivity networks for salience processing and executive control. *J. Neurosci.* **27**, 2349–2356 (2007).
57. V. Menon, L. Q. Uddin, Saliency, switching, attention and control: A network model of insula function. *Brain Struct. Funct.* **214**, 655–667 (2010).
58. E. J. Hermans, *et al.*, Stress-related noradrenergic activity prompts large-scale neural network reconfiguration. *Science* **334**, 1151–1153 (2011).
59. B. Roozendaal, E. J. Hermans, Norepinephrine effects on the encoding and consolidation of emotional memory: Improving synergy between animal and human studies. *Curr. Opin. Behav. Sci.* **14**, 115–122 (2017).
60. E. R. Samuels, E. Szabadi, Functional neuroanatomy of the noradrenergic locus coeruleus: Its roles in the regulation of arousal and autonomic function. Part I: Principles of functional organisation. *Curr. Neuropharmacol.* **6**, 235–253 (2008).
61. K. A. Coffman, R. P. Dum, P. L. Strick, Cerebellar vermis is a target of projections from the motor areas in the cerebral cortex. *Proc. Natl. Acad. Sci. U.S.A.* **108**, 16068–16073 (2011).
62. D. J.-F. de Quervain *et al.*, A deletion variant of the α2b-adrenoceptor is related to emotional memory in Europeans and Africans. *Nat. Neurosci.* **10**, 1137–1139 (2007).
63. D. J.-F. de Quervain *et al.*, PKCα is genetically linked to memory capacity in healthy subjects and to risk for posttraumatic stress disorder in genocide survivors. *Proc. Natl. Acad. Sci. U.S.A.* **109**, 8746–8751 (2012).
64. Y. L. Mertens, A. Manthey, A. Sierk, H. Walter, J. K. Daniels, Neural correlates of acute post-traumatic dissociation: A functional neuroimaging script-driven imagery study. *BJPsych Open* **8**, e109 (2022).
65. A. Tavano *et al.*, Disorders of cognitive and affective development in cerebellar malformations. *Brain* **130**, 2646–2660 (2007).
66. E. Courchesne, R. Yeung-Courchesne, G. A. Press, J. R. Hesselink, T. L. Jernigan, Hypoplasia of cerebellar vermal lobules VI and VII in autism. *N. Engl. J. Med.* **318**, 1349–1354 (1988).
67. D. Q. Beversdorf *et al.*, The effect of semantic and emotional context on written recall for verbal language in high functioning adults with autism spectrum disorder. *J. Neurol. Neurosurg. Psychiatry* **65**, 685–692 (1998).
68. C. Deruelle, B. Hubert, A. Santos, B. Wicker, Negative emotion does not enhance recall skills in adults with autistic spectrum disorders. *Autism Res.* **1**, 91–96 (2008).
69. M. L. Bauman, T. L. Kemper, Neuroanatomic observations of the brain in autism: A review and future directions. *Int. J. Dev. Neurosci.* **23**, 183–187 (2005).
70. S. Baron-Cohen *et al.*, The amygdala theory of autism. *Neurosci. Biobehav. Rev.* **24**, 355–364 (2000).
71. C. J. Stoodley, J. D. Schmahmann, Evidence for topographic organization in the cerebellum of motor control versus cognitive and affective processing. *Cortex* **46**, 831–844 (2010).
72. A. Heck *et al.*, Converging genetic and functional brain imaging evidence links neuronal excitability to working memory, psychiatric disease, and brain activity. *Neuron* **81**, 1203–1213 (2014).
73. G. Luksys *et al.*, Computational dissection of human episodic memory reveals mental process-specific genetic profiles. *Proc. Natl. Acad. Sci. U.S.A.* **112**, E4939–E4948 (2015).
74. P. J. Lang, M. M. Bradley, B. N. Cuthbert, *International Affective Picture System (IAPS): Affective Ratings of Pictures and Instruction Manual* (Technical, 2005).
75. J. Ashburner, A fast diffeomorphic image registration algorithm. *Neuroimage* **38**, 95–113 (2007).
76. A. Klein *et al.*, Evaluation of 14 nonlinear deformation algorithms applied to human brain MRI registration. *Neuroimage* **46**, 786–802 (2009).
77. S. J. Kiebel, S. Klöppel, N. Weiskopf, K. J. Friston, Dynamic causal modeling: A generative model of slice timing in fMRI. *Neuroimage* **34**, 1487–1496 (2007).
78. R. Sladky *et al.*, Slice-timing effects and their correction in functional MRI. *Neuroimage* **58**, 588–594 (2011).
79. A. P. Leff *et al.*, The cortical dynamics of intelligible speech. *J. Neurosci.* **28**, 13209–13215 (2008).
80. M. L. Seghier, C. J. Price, Reading aloud boosts connectivity through the putamen. *Cereb. Cortex* **20**, 570–582 (2010).
81. F. M. Richardson, M. L. Seghier, A. P. Leff, M. S. C. Thomas, C. J. Price, Multiple routes from occipital to temporal cortices during reading. *J. Neurosci.* **31**, 8239–8247 (2011).
82. W. D. Penny, K. E. Stephan, A. Mechelli, K. J. Friston, Modelling functional integration: A comparison of structural equation and dynamic causal models. *Neuroimage* **23**, S264–S274 (2004).
83. J. Daunizeau, O. David, K. E. Stephan, Dynamic causal modelling: A critical review of the biophysical and statistical foundations. *Neuroimage* **58**, 312–322 (2011).
84. K. J. Friston, B. Li, J. Daunizeau, K. E. Stephan, Network discovery with DCM. *Neuroimage* **56**, 1202–1221 (2011).
85. K. J. Friston, Functional and effective connectivity: A review. *Brain Connect.* **1**, 13–36 (2011).
86. A. C. Marreiros, S. J. Kiebel, K. J. Friston, Dynamic causal modelling for fMRI: A two-state model. *Neuroimage* **39**, 269–278 (2008).
87. D. A. Berry, Y. Hochberg, Bayesian perspectives on multiple comparisons. *J. Stat. Plan. Inference* **82**, 215–227 (1999).
88. K. J. Friston, W. Penny, Posterior probability maps and SPMs. *Neuroimage* **19**, 1240–1249 (2003).

89. H. Hillebrandt, I. Dumontheil, S.-J. Blakemore, J. P. Roiser, Dynamic causal modelling of effective connectivity during perspective taking in a communicative task. *Neuroimage* **76**, 116–124 (2013).
90. Z. Gu, L. Gu, R. Eils, M. Schlesner, B. Brors, Circlize implements and enhances circular visualization in R. *Bioinformatics* **30**, 2811–2812 (2014).
91. B. Fischl *et al.*, Whole brain segmentation: Automated labeling of neuroanatomical structures in the human brain. *Neuron* **33**, 341–355 (2002).
92. R. S. Desikan *et al.*, An automated labeling system for subdividing the human cerebral cortex on MRI scans into gyral based regions of interest. *Neuroimage* **31**, 968–980 (2006).
93. D. Coynel, Human cerebellum and corticocerebellar connections involved in emotional memory enhancement. Open Science Framework. https://osf.io/ghtvy. Deposited 14 September 2022.
94. D. Coynel, Data from "Human cerebellum and corticocerebellar connections involved in emotional memory enhancement." Figshare. https://figshare.com/projects/CB-DCM/149317. Deposited 21 September 2022.
95. D. Coynel, Human cerebellum and corticocerebellar connections involved in emotional memory enhancement. Neurovault. https://neurovault.org/collections/12932. Deposited 14 September 2022.